JOURNAL OF GEOPHYSICAL RESEARCH, VOL. 114, D23305, doi:10.1029/2009JD011997, 2009

Validation of ground-based microwave radiometers at 22 GHz for stratospheric and mesospheric water vapor

A. Haefele,[1] E. De Wachter,[1] K. Hocke,[1,2] N. Kämpfer,[1,2] G. E. Nedoluha,[3] R. M. Gomez,[3] P. Eriksson,[4] P. Forkman,[4] A. Lambert,[5] and M. J. Schwartz[5]

Received 3 March 2009; revised 22 July 2009; accepted 29 July 2009; published 8 December 2009.

[1] We present a detailed intercomparison of five ground-based 22 GHz microwave radiometers for stratospheric and mesospheric water vapor. Four of these instruments are members of the Network for the Detection of Atmospheric Composition Change (NDACC). The global measurements of middle atmospheric water vapor of the Microwave Limb Sounder (MLS) onboard the Aura satellite serve as reference and allow intercomparison of the ground-based systems that are located between 45°S and 57°N. The retrievals of water vapor profiles from the ground-based radiation measurements have been made consistent to a large extent: for the required temperature profiles, we used the global temperature measurements of MLS and we agreed on one common set of spectroscopic parameters. The agreement with the reference measurements is better than ±8% in the altitude range from 0.01 to 3 hPa. Strong correlation is found between the ground-based and the reference data in the mesosphere with respect to seasonal cycle and planetary waves. In the stratosphere the measurements are generally more noisy and become sensitive to instrumental instabilities toward lower levels (pressures greater than 3 hPa). We further present a compilation of a NDACC data set based on the retrieval parameters described herein but using a temperature climatology derived from the MLS record. This makes the ground-based measurements independent of additional information and allows extension of the data set for years in a homogeneous manner.

Citation: Haefele, A., E. De Wachter, K. Hocke, N. Kämpfer, G. E. Nedoluha, R. M. Gomez, P. Eriksson, P. Forkman, A. Lambert, and M. J. Schwartz (2009), Validation of ground-based microwave radiometers at 22 GHz for stratospheric and mesospheric water vapor, *J. Geophys. Res.*, *114*, D23305, doi:10.1029/2009JD011997.

1. Introduction

[2] The main source of water vapor in the atmosphere is the evaporation from the Earth's surface. Water vapor enters the stratosphere through the tropical tropopause, which acts as a cold trap and renders the stratosphere and mesosphere typically a thousand times dryer than the lower troposphere. Methane oxidation is the second important source of water vapor in the stratosphere and provides a link between stratospheric humidity and human activities [*Forster et al.*, 2007]. As the dominant greenhouse gas, water vapor has a strong impact on the radiative budget of the atmosphere and hence on the Earth's surface temperature. The long lifetime of water vapor in the stratosphere makes it a good tracer and gives valuable information about the atmospheric circulation and waves.

[3] Water vapor in the upper stratosphere and mesosphere is mainly observed by spaceborne and ground-based remote sensing instruments in passive modes. While single ground-based instruments cannot provide any information on the horizontal distribution of water vapor, they are characterized by long operational lifetimes. They are hence of major importance for water vapor monitoring and for the intercomparison of consecutive satellite missions. The merging of data sets of consecutive satellite missions is an important task to generate global and homogeneous long-term data sets that are essential for the climate community. A network of ground-based instruments allows to detect biases between satellite experiments as well as the geographical dependence of these biases and plays a key role in the attempt to merge satellite data sets. A good characterization of the uncertainties, long-term stability and consistency are key requirements for a network in this respect. Consistency means that measurements of the individual instruments of the network are in agreement with each other in terms of absolute values and in terms of information content. This has been formulated by *Harris* [1976] as follows: "It therefore seems imperative that workers [..] should combine to compare their instrumental sensitivities and errors so that some standardization

[1]Department of Microwave Physics, Institute of Applied Physics, University of Bern, Bern, Switzerland.
[2]Oeschger Center for Climate Change Research, University of Bern, Bern, Switzerland.
[3]Naval Research Laboratory, Washington, D. C., USA.
[4]Department of Radio and Space Science, Chalmers University of Technology, Gothenburg, Sweden.
[5]Jet Propulsion Laboratory, California Institute of Technology, Pasadena, California, USA.

0148-0227/09/2009JD011997$09.00

of results may be achieved. Without such standardization, much information about the real nature and behavior of stratospheric humidity is being lost."

[4] At the time of writing several new ground-based 22 GHz radiometers for middle atmospheric water vapor are being developed [*Motte et al.*, 2007; *Straub et al.*, 2008] and the network of such instruments will increase in the near future. There is thus a need for a standardization of the data reduction to increase the significance of data intercomparisons and to retrieve the highest amount of information from the network.

[5] In this paper we present an intercomparison of five ground-based microwave radiometers for middle atmospheric water vapor that are members of the Network for the Detection of Atmospheric Composition Change (NDACC). The global data set of middle atmospheric water vapor of the Earth Observing System (EOS) Microwave Limb Sounder (MLS) serves as reference and allows to perform an intercomparison of the ground-based instruments that are located at different sites. The retrievals of the radiometer systems have been standardized to a large extent: Temperature information, that is required in the water vapor retrieval, is taken from the global temperature record of MLS. Also, a common set of spectroscopic parameters has been used.

[6] The paper is organized as follows: The intercomparison strategy is elucidated in section 2. In sections 3 and 4 the ground-based instruments and the space-borne MLS, respectively, are introduced. Section 5 is dedicated to the retrieval of water vapor profiles from measured radiation spectra. In sections 6 and 7 we present and discuss the results and implications of the intercomparison.

2. Intercomparison Strategy

[7] In order to compare measurements of ground-based instruments that are not located at the same place a reference measurement is needed that is available at each location. Under the assumption that the reference measurement does not have a location-dependent bias it is then possible to estimate differences between the instruments under consideration from the differences between the instruments and the reference according to the approach of the double differences by *Hocke et al.* [2007]. As a traveling standard for ground-based microwave radiometry is not yet available we have chosen the Microwave Limb Sounder (MLS) on board of the Aura satellite (see section 4) as the reference for this study because its water vapor product has extensively been validated [*Lambert et al.*, 2007; *Nedoluha et al.*, 2007; *Vömel et al.*, 2007] and has proven to be of good quality. Furthermore the data set shows excellent continuity and covers the latitudes up to 82° north and south.

[8] The retrieval of a water vapor profile from a measured spectrum requires a first guess of the H_2O profile and its error, i.e., the a priori profile and its covariance, auxiliary information like pressure and temperature profiles and a forward model that does the radiative transfer calculations and establishes a relation between an atmospheric state and the measured intensity spectrum. These retrieval parameters are generally chosen in an attempt to optimize the retrievals from a particular type of instrument, and the specific choice can affect the retrieved water vapor values significantly. All of the retrievals of this study use a common set of retrieval parameters to eliminate biases between the instruments that simply originate from differences in the spectroscopic parameters or in the temperature information, for instance. A detailed description of the applied inversion parameters and their values is given in section 5.

3. Instruments

[9] The five microwave radiometers under consideration are operated at the four NDACC sites Onsala (57°N, 12°E, 50 m amsl), Bern (47°N, 7°E, 900 m amsl), Mauna Loa (20°N, 156°W, 3500 m amsl) and Lauder (45°S, 170°E, 200 m amsl), and at Seoul (37°N, 127°E, 50 m amsl), which is not a NDACC site yet. The geographical distribution of the radiometers is shown in Figure 1. All systems measure the rotational transition line of H_2O at 22.235 GHz in a balancing mode including a line measurement at a low elevation angle (20°–40°) and a reference measurement in zenith direction according to the method first introduced by *Parrish et al.* [1988]. Small modifications, however, are made and for details we refer to the instrument papers referenced in Table 1. The receiver front ends consist of a horizontally aligned horn antenna and a rotating mirror at 45° inclination allowing the beam to be pointed at different elevation angles. The optical components are followed by a heterodyne receiver which amplifies the incoming signal and converts it to a lower frequency range to be analyzed by a spectrometer. Important specifications and references of the five systems are given in Table 1.

[10] In the hot-cold calibration mode, that is applied by three of the five instruments (Onsala, Bern and Seoul), the atmospheric signal is compared to the signals from two reference targets at known temperatures. The hot load, which is a microwave absorber at ambient temperature, and the cold load, which is the sky itself. The temperature of the sky and the opacity of the atmosphere are derived on regular intervals of 30 min from a tipping curve measurement [*Han and Westwater*, 2000]. The tipping curve is a set of atmospheric measurements taken at different elevation angles to which a model of the atmosphere is fitted with its opacity as a free parameter revealing both τ and the temperature of the sky. The noise diode calibration mode, applied at Lauder and Mauna Loa, uses a noise diode as reference and its temperature is determined on a weekly basis by means of a hot-cold calibration using an ambient temperature and a liquid nitrogen calibration load. The atmospheric opacity is derived from tipping curve measurements as well.

[11] The Water Vapor Millimeter wave Spectrometers (WVMS) at Mauna Loa and Lauder have been in operation since 1996 and 1992, respectively, and have undergone extensive validation (see references in Table 1). The Onsala and Bern systems started operation in 2002. The instrument from Bern showed drifts in the properties of the previously used acousto-optical spectrometer before March 2007 and we will present only data after the implementation of a new digital FFT spectrometer in March 2007. The Stratospheric Water vapor RAdiometer (SWARA) began with routine measurements in October 2006. Features in the spectra that originated from a frequency dependence in the antenna

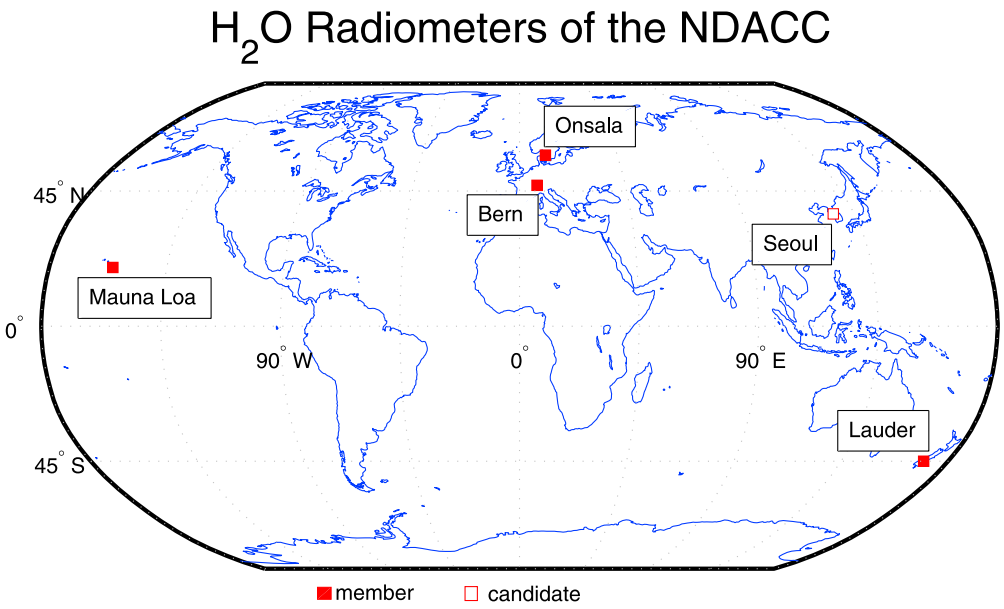

Figure 1. Location of the five 22 GHz radiometers for middle atmospheric water vapor.

pattern strongly limited the practical bandwidth and hence do not allow to retrieve water vapor below 1 hPa [*De Wachter et al.*, 2009]. This problem has been solved but at the time of this work there was no new data version available and we will thus not show any data from Seoul for pressures greater than 1 hPa.

4. MLS

[12] Because the temperature as well as the water vapor product of the Earth Observing System Microwave Limb Sounder (EOS MLS), herein after referred to as MLS, are extensively used in this study we give here a short overview of this instrument. MLS is operated on board of the Aura satellite that was launched 15 July 2004, and is part of NASA's A-train group, which is a formation of six satellites flying in close proximity. The Aura satellite is on a near polar orbit covering 82°S to 82°N latitudes. The measurements are taken at fixed local solar times. A detailed description of MLS is given by *Waters et al.* [2006].

[13] MLS observes thermal microwave emission by the atmosphere in five spectral regions from 115 GHz to 2.5 THz. The Earth's limb is scanned vertically from the ground to 96 km. These scans are synchronized to the Aura orbit such that vertical scans are made at essentially the same latitudes each orbit.

[14] Temperature is derived from observations near the 118 GHz O_2 spectral line and the 243 GHz $O^{18}O$ spectral line. The vertical resolution of the MLS temperature measurement, taken to be the full width at half maximum of the averaging kernels, is 4 km at 10 hPa, 8 km at 1 hPa, 9 km at 0.1 hPa, 14 km at 0.01 hPa and 15 km at 0.001 hPa. In the horizontal along-track direction, the temperature data have single profile resolution of 165 km through most of the profile, degrading to 185 km at 0.01 hPa and to 220 km at 0.001 hPa [*Schwartz et al.*, 2008]. [*Schwartz et al.*, 2008] present a detailed validation of the MLS temperature data version 2.2 and report a cold bias of 1–3 K compared to SABER, ACE and HALOE in the upper stratosphere and mesosphere. Regarding the error in the water vapor retrieval of the ground-based instruments with respect to an error in the temperature profile of −2%/5 K (see section 5.5), the cold bias in MLS temperatures leads to an overestimation of water vapor of <1.5%. The seasonal and latitudinal dependence of the bias in MLS temperatures with respect to SABER temperatures is <3 K up to 0.1 hPa between 50°S and 50°N [*Schwartz et al.*, 2008].

Table 1. Key Specifications of the Five Microwave Radiometers for Stratospheric and Mesospheric Water Vapor[a]

	Onsala[b]	Bern[c]	Seoul	Mauna Loa[d]	Lauder[d]
Project name		MIAWARA	SWARA	WVMS-3	WVMS-1
Spectrometer	autocorrelator	digital FFT	digital FFT	filter bank	filter bank
Spectral resolution	25 kHz	61 kHz	61 kHz	50 kHz	200 kHz
Bandwidth	20 MHz	100 MHz	15 MHz	60 MHz	40 MHz
Receiver temperature	170 K	135 K	140 K	170 K	100 K
Preamplifier (HEMT)	uncooled	uncooled	uncooled	cooled	cooled
Calibration	hot-cold	hot-cold	hot-cold	noise diode	noise diode

[a]The spectral resolution refers to the best resolution at line center.
[b]From *Forkman et al.* [2003].
[c]From *Deuber et al.* [2004, 2005].
[d]From *Thacker et al.* [1995] and *Nedoluha et al.* [1995, 1997, 2007].

Table 2. Description of Variables Used in the Optimal Estimation Retrieval of H_2O Profiles

Variable	Description
$\mathbf{y}$	measured spectrum at frequencies depending on spectrometer
$F(\mathbf{x})$	calculated spectrum based on an atmospheric state $\mathbf{x}$
$\mathbf{K}$	derivative of F with respect to $\mathbf{x}$
$\mathbf{x}$	the true atmospheric state
$\mathbf{x_a}$	a priori assumption of the atmospheric state, i.e., of the H_2O distribution
$\hat{\mathbf{x}}$	the retrieved atmospheric state
$\mathbf{S_y}$	error covariance matrix of the measured spectrum
$\mathbf{S_a}$	error covariance matrix of the a priori assumption

[15] Water vapor profiles are retrieved from the limb emission measurements at 183.31 GHz. The vertical resolution is better than 4 km below the stratopause and increases to >10 km in the mesosphere and the along-track horizontal resolution is on the order of 400 km [*Lambert et al.*, 2007]. *Lambert et al.* [2007] present a detailed validation of the MLS H_2O product and report a bias compared to ACE-FTS of ±5% for pressures 68–0.004 hPa and a bias compared to HALOE of +2% to +10% for pressures 68–1.5 hPa. The precision on individual profiles is 0.4 ppmv at 0.1 hPa, 0.3 ppmv at 1 hPa and 0.2 ppmv at 10 hPa. No latitudinal dependence of the biases is reported. This is of particular importance for this study as MLS serves as reference for the ground-based instruments that are spread between 45°S and 58°N.

5. Retrieval

5.1. Optimal Estimation Algorithm

[16] The forward model implements a radiative transfer calculation and provides the relation between an atmospheric state and a measured spectrum, accounting also for instrumental properties like antenna pattern, side band suppression or spectrometer resolution. The inverse problem is the derivation of the atmospheric state from a measured radiation spectrum. It is ill posed, which means that an infinite number of solutions exists. A statistical approach is used to find the most likely atmospheric state given a measured radiation spectrum. For the ground-based instruments we used the optimal estimation method by *Rodgers* [1976], which minimizes the following cost function derived from Bayes' theorem:

$$c = [\mathbf{y} - F(\hat{\mathbf{x}})]^T \mathbf{S_y^{-1}} [\mathbf{y} - F(\hat{\mathbf{x}})] + [\hat{\mathbf{x}} - \mathbf{x_a}]^{\mathbf{T}} \mathbf{S_a^{-1}} [\hat{\mathbf{x}} - \mathbf{x_a}]. \quad (1)$$

The variables are described in Table 2.

[17] Costs are generated by deviations from the measured spectrum in the observation space, $\mathbf{y}-F(\hat{\mathbf{x}})$, weighted with the inverse covariance of the measurement, $\mathbf{S_y}$, and by deviations from the a priori estimate in the state space, $\hat{\mathbf{x}} - \mathbf{x_a}$, accordingly weighted by the inverse a priori covariance, $\mathbf{S_a}$. The second term constrains the solution to physically meaningful states.

[18] The low concentration of water vapor in the stratosphere and mesosphere allows to use the linearization,

$$F(\hat{\mathbf{x}}) \simeq F(\mathbf{x_a}) + \mathbf{K}(\hat{\mathbf{x}} - \mathbf{x_a}), \quad (2)$$

where $\mathbf{K}$ is the partial derivative of F with respect to $\mathbf{x}$. Inserting (2) in (1) and solving $dc/d\hat{\mathbf{x}} = 0$ for $\hat{\mathbf{x}}$ yields

$$\hat{\mathbf{x}} = \mathbf{x_a} + \left(\mathbf{S_a^{-1}} + \mathbf{K^T S_y^{-1} K}\right)^{-1} \mathbf{K^T S_y^{-1}} (\mathbf{y} - F(\mathbf{x_a})). \quad (3)$$

The retrieved profile thus consists of an a priori estimate to which we add a fraction of the H_2O profile corresponding to $(\mathbf{y} - F(\mathbf{x_a}))$. The amount of information that is added to $\mathbf{x_a}$ depends on the error covariances of $\mathbf{x_a}$ and $\mathbf{y}$, namely $\mathbf{S_a}$ and $\mathbf{S_y}$, and on the kernel $\mathbf{K}$ which describes the physical sensitivity of the spectrum to changes in $\mathbf{x}$. $\mathbf{K}$ approaches zero at low pressures (high altitudes) where the absolute amount of H_2O becomes very small and where the line width becomes smaller than the spectral resolution of the instrument. For the five instruments the level where the contribution of the measurement becomes smaller than 60% lies typically between 70 and 80 km.

[19] Also, $\mathbf{K}$ decreases at high pressures (low altitudes), where the line width becomes larger than the bandwidth of the instrument due to the pressure broadening. In practice, the lower boundary for valid water vapor retrievals lies much higher than the theoretical value due to spectral artifacts from internal reflections. These artifacts are often referred to as "baselines" and are sine wave like structures that are superimposed on the spectrum. Baselines are accounted for in the forward model with an empirically determined set of sine waves of one or more known periods, or a polynomial fit of low order to the measured spectrum. Variations over time in the baseline cause unnatural variability in the retrieved water vapor values mainly at the lower levels. For the five instruments the lower boundary where the measurements are reliable lies between 1 and 3 hPa. For some instruments special retrieval setups allow retrievals to reach 10 hPa, but this is not further discussed here. The instruments from Onsala, Bern and Seoul use the retrieval software package QPack that is a user friendly implementation of the optimal estimation retrieval [*Eriksson et al.*, 2005].

[20] In sections 5.3 to 5.6 the most important retrieval parameters are discussed.

5.2. Averaging Kernels

[21] The averaging kernel, $\mathbf{A}$, characterizes the response of the retrieved profile to a perturbation in the true profile: $\mathbf{A} = \partial\hat{\mathbf{x}}/\partial\mathbf{x}$. It accounts for the limited vertical resolution and, at least as important, for the sensitivity of the retrieval that decreases toward higher and lower altitudes. $\mathbf{A}$ depends upon the measurement covariance matrix, $\mathbf{S_y}$. To account for possible variations in the signal to noise ratio that is given by $\mathbf{S_y}$ the averaging kernels are calculated for each retrieved profile. To derive the profile as it would be measured by the radiometer system, $\hat{\mathbf{x}}_{\mathbf{ref}}$, from a colocated reference profile, $\mathbf{x_{ref}}$, the averaging kernels are considered as follows:

$$\hat{\mathbf{x}}_{\mathbf{ref}} = \mathbf{x_a} + \mathbf{A}(\mathbf{x_{ref}} - \mathbf{x_a}). \quad (4)$$

If not mentioned otherwise the MLS water vapor data are convolved with the averaging kernels of the microwave systems according to equation (4) where $\mathbf{x_a}$ is the a priori

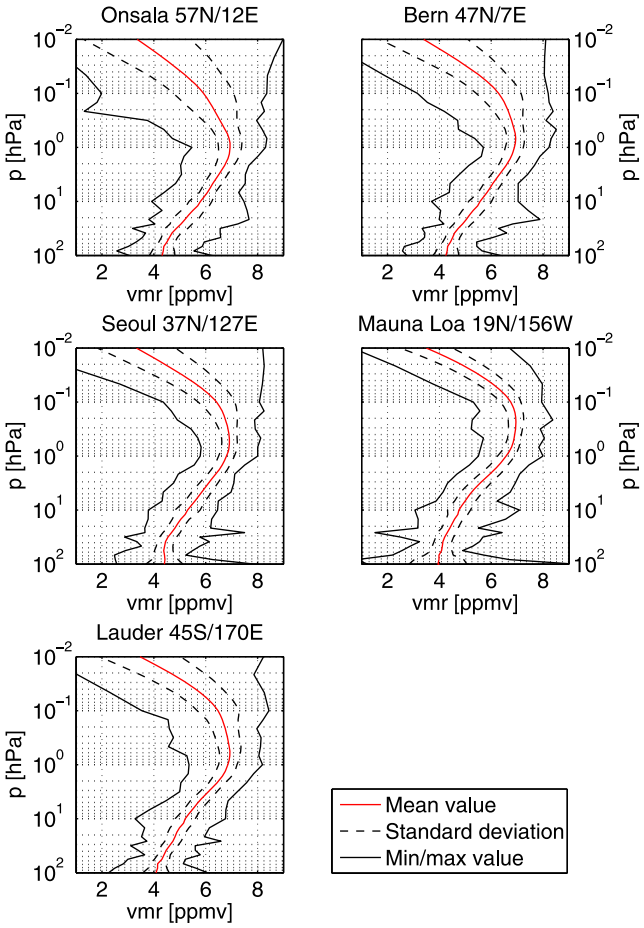

Figure 2. Mean MLS profiles of the time period from August 2004 to September 2009. These profiles were used as a priori profiles in the retrievals of the ground-based instruments.

profile of the ground-based instrument. The vertical resolution of MLS at 0.10 hPa is better by a factor of 2 than that of the ground-based instruments and is being neglected.

5.3. A Priori Information on H_2O

[22] Given the strong latitudinal dependence of the vertical distribution and the variability of middle atmospheric water vapor, it is not appropriate to use one single a priori profile in the retrievals of all instruments in the attempt to establish similar conditions for the retrievals of all instruments. Instead, individual a priori profiles were constructed for each instrument site by taking the mean of all MLS H_2O profiles within 200 km in latitude and 400 km in longitude from the period 2004–2008. A smoothing has subsequently been applied to get rid of oscillations in the mean MLS H_2O profiles. The a priori profiles of each site are presented in Figure 2. The fact that mean MLS water vapor profiles are used as a priori profiles in the retrievals, which are subsequently compared to MLS measurements, is not an issue, since the comparison is restricted to the altitude ranges where the contribution of the a priori profile is very low. By using a priori profiles that are constant in time we assure that all the seasonal variations in the H_2O retrievals come from the measurements.

[23] The a priori covariance matrix, $\mathbf{S_a}$, defines the error of the a priori profile and controls the strength of the constraint of the retrieved profile to the a priori profile. The covariance matrix is defined by the standard deviation, σ, on each pressure level and the correlation length, l_c, giving the distance over which the correlation between two levels decreases below 30%. The correlation is assumed to follow a Gaussian curve. The choice for the values for σ and l_c is only partially motivated by the numbers derived from observational data sets but also by the requirement for a stable and sensitive retrieval. The covariance matrices are thus specific for each instrument but this can be accepted as $\mathbf{S_a}$ has only a minor influence on the bias of the retrieved water vapor data. The values for σ and l_c that were used in the retrievals are given in Table 3.

5.4. Spectroscopy

[24] In order to compute the atmospheric emission due to a given transition of a given molecule the absorption coefficient has to be calculated as a function of frequency. The four essential line parameters are the resonant frequency, ν_0, the line intensity, $S(T)$, the line width, $\Delta_\nu(p, T)$, and the energy of the lower quantum state, E''. The line width accounts for the natural, Doppler and pressure broadening of the spectral line and the latter requires a further set of parameters consisting of the self and air broadening parameters, γ_{air} and γ_{self}, accounting for water-air and water-water collisions, respectively, and of the exponents for the temperature dependence, n_{air} and n_{self}, respectively. The pressure broadened line half-width $\Delta\nu(p, T)$ for a gas at pressure p, temperature T and partial pressure p_s is given by

$$\Delta\nu(p,T) = \left(\frac{T_{ref}}{T}\right)^{n_{air}} \gamma_{air}(p - p_s) + \left(\frac{T_{ref}}{T}\right)^{n_{self}} \gamma_{self} p_s. \quad (5)$$

Values for all of these parameters base on measurements or calculations or both and are provided by spectral catalogues like JPL or HITRAN and by a wealth of publications. Table 4 shows a selection of values that can be found in the literature. For our study we used the broadening parameters from *Liebe* [1989], the line intensity, lower state energy and the line center frequency from the JPL 1985 catalogue [*Poynter and Pickett*, 1985]. These values are used in the WVMS retrievals since 1992 and reveal good validation results and are hence well suited for this study as well. In the context of a network, the consistency resulting from the use of a common set of values is more important than the absolute values. A Voigt line shape accounts for

Table 3. Parameters of the a Priori Covariance Matrices[a]

	Onsala		Bern and Seoul		Mauna Loa and Lauder	
p (hPa)	σ	l_c	σ	l_c	σ	l_c
10	1.53	3	0.6	4	1.5	0
3	1.53	3	0.6	4	1.5	0
1	1.53	3	0.7	4	1.5	0
0.3	1.53	3	0.8	4	1.5	0
0.1	1.53	3	1.1	4	1.5	0
0.03	1.53	3	1.6	4	1.5	0
0.01	1.53	3	1.7	4	1.5	0

[a]The standard deviation, σ, is given in ppmv, and the correlation length, l_c, is given in kilometers. The correlation is assumed to follow a Gaussian curve (see section 5.3).

Table 4. Spectroscopic Parameters of the $6_{16}-5_{23}$ Transition of H_2O for $T = 296$ K[a]

	ν_0 (GHz)	S (m^2Hz)	E'' (J)	γ_{air} (Hz/Pa)	n_{air}	γ_{self} (Hz/Pa)	n_{self}
HITRAN 2004[b]	22.2353067	1.3173e-18	8.86970e-21	27871	0.640	105538	
JPL 2001[c]	22.2350800	1.3304e-18	8.86970e-21				
JPL 1985[d]	**22.2350800**	**1.3206e-18**	**8.86987e-21**				
Cazzoli et al. [2007]				25978	0.760	124961	1.23
Payne et al. [2008]				26628			
Liebe [1989]	22.2350800			**28110**	**0.690**	**134928**	**1**

[a]Notation: ν_0, resonant frequency; S, line intensity; γ_{air} (γ_{self}), air (self) broadening parameter; n_{air} (n_{self}), temperature dependence of γ_{air} (γ_{self}). The boldface values have been used for all retrievals in this study.
[b]*Rothman et al.* [2005].
[c]*Cohen et al.* [1998].
[d]*Poynter and Pickett* [1985].

pressure and Doppler broadening. For the Mauna Loa and Lauder systems an adapted version of the radiative transfer model by *Liebe* [1989] is used while the Atmospheric Radiative Transfer Simulator (ARTS) [*Buehler et al.*, 2005] is used for the other systems.

5.5. Temperature Information

[25] The emission of the atmosphere depends on the actual temperature profile. Underestimating the temperature at a particular level will cause the retrieval to overestimate the water vapor amount required to emit the observed signal. The relative error in H_2O mixing ratio depends on altitude and is on the order of −2%/5 K. For the retrievals of the ground-based microwave systems the temperature profiles are routinely taken from different analyses as provided by NCEP, ECMWF or from models or climatologies like WACCM or MSISE90. But upper stratospheric and mesospheric temperature data provided by analyses or models are purely modeled and afflicted with considerable uncertainties. Observations as provided by SABER or MLS for an extended altitude range are assumed to be a better data source. *Nedoluha et al.* [2007] investigated the performance of MLS temperature observations in the WVMS retrievals, and reported an improvement in the reanalyzed water vapor retrievals mainly with respect to interannual variations. In this study the MLS temperature observations at the specific locations were used in the retrievals for all microwave systems and hence the validation is free of effects that are related to the use of different temperature data sources.

[26] As a consequence of the Sun-synchronous orbit, the MLS measurements are taken at constant local solar times, with daytime measurements on the ascending branch. Because of the coincidence criterion (see section 6) and data availability there are not always both day and nighttime measurements available at one site for a 24 h interval. This can introduce biases in daily mean profiles as differences between day and nighttime measurements are on the order of 5 K at 0.10 hPa. To create data sets of daily temperature profiles that are more representative for 24 h we thus calculated 3 day running means where day and nighttime measurements were equally weighted, for example, the mean of the mean daytime and the mean nighttime profile of a 72 h interval.

5.6. Measurement Integration Time

[27] As the tropospheric opacity attenuates the signal from the middle atmosphere it has a major influence on the signal to noise ratio of the ground-based measurements. The instruments are located between 45°S and 57°N and at altitudes from 50 to 3400 amsl and thus encounter very different conditions in terms of opacity. Figure 3 shows the mean annual cycle of the tropospheric opacity at the different sites. The signal to noise ratio governs the contribution of the a priori profile to the retrieval and must be kept constant. This in turn requires longer integration times for higher opacities. In Onsala, Bern and Seoul the number of spectra to be averaged before a retrieval depends on the actual value of the opacity to conserve the signal to noise ratio. Thus, the time between two retrievals changes dramatically with season; at Seoul the integration time ranges from a couple of hours in winter up to 4 weeks in summer. On the other hand, at Mauna Loa and Lauder a constant number of 500 spectra (∼1 week) is averaged before being fed into the inversion routine. Such a long integration time and the rather low opacities encountered at Mauna Loa and Lauder lead to a reasonably constant signal to noise ratio throughout the whole year.

[28] Due to the nonlinearity of the radiative transfer, the inversion of a mean spectrum is not the same as the mean of the retrievals from the individual spectra. The systematic bias due to the combined effect of nonlinearity of the radiative transfer and long integration times was found to be <0.25% up to the 0.01 hPa level (based on simulations) and is further neglected in this study. Furthermore, an integration time of one day and more reduces the effect of daily variations of water vapor on the comparison. However, diurnal variations are expected to have an amplitude of less than 1% up to 65 km [*Haefele et al.*, 2008] and should not significantly affect the comparison. Also, any bias arising from the

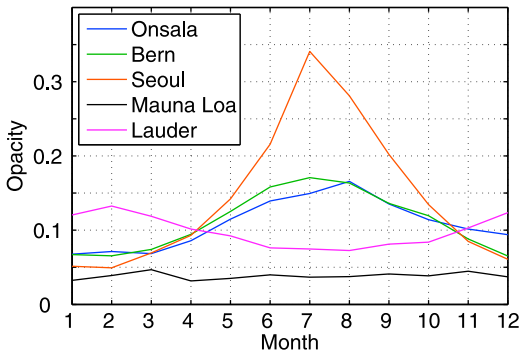

Figure 3. Monthly means of the tropospheric opacity at 22.235 GHz at the different sites.

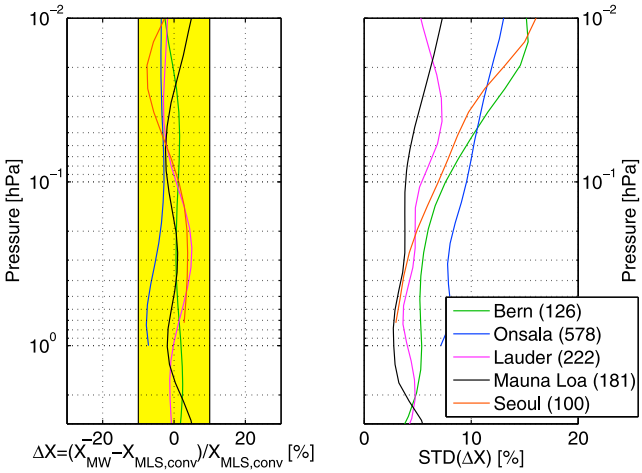

Figure 4. (left) Mean value and (right) standard deviation of the relative differences between the ground-based measurements and the reference data (MLS). The numbers in brackets in the legend indicate the number of available profile pairs at each site.

MLS sampling at fixed local solar times is hence expected to be of minor importance.

[29] While statistical errors like noise can be reduced by longer integration times, this does no apply for systematic errors. But systematic spectral errors are much smaller than the standard deviation of the target noise for all instruments and are not further discussed here. One exception, however, are baselines, which are features in the measured spectrum that originate from internal reflections. The structure of baselines is usually well known and they are thus not treated as spectral errors but included in the forward model (see section 5.1). However, if the baseline is not well known or if it changes over time, baselines may affect the retrievals and can lead to unrealistic fluctuations (see section 6).

6. Intercomparison of the Ground-Based Measurements

[30] For each ground-based retrieval a correlative MLS profile is generated by taking the mean profile of all MLS measurements that are available within ±200 km in latitude and ±400 km in longitude and within the integration time necessary for the ground-based observation (hours to days). With this approach we get the following totals of coincidences: Onsala: 578, Bern: 128, Seoul: 109, Mauna Loa: 186 and Lauder: 224. We then calculated the differences between the ground-based retrievals and the correlative MLS profiles. The mean values and the standard deviations of these differences are presented in Figure 4 and the corresponding time series are presented in Figure 5 and 6. The agreement between the ground-based instruments and the reference is better than 8% in the whole altitude range.

[31] The biases of the Mauna Loa and Lauder instruments with respect to MLS are on average between −3 and 3% and between −3 and 5%, respectively, and the standard deviations are lower than 7% for both instruments, indicating very good correlation with the reference data. However, the decrease of the standard deviation of the Lauder data above 0.04 hPa is related to the increase of the a priori contribution which in turn is a consequence of the degradation of the averaging kernels due to the limited spectral resolution (see section 5.1). These values are in agreement with those reported by *Nedoluha et al.* [2007].

[32] The Bern instrument agrees with MLS within −3 to 3%. Unlike the other instruments under consideration, we found a wet bias of 2% between 0.20 and 0.03 hPa for this instrument. This wet bias, however, is only apparent during the summer season, particularly during summer 2007 (see Figure 5). If only the winter months (10–5) are considered the same analysis reveals a mean difference of −2% between 0.10 and 0.03 hPa in excellent agreement with the WVMS instruments and the Onsala system. The Seoul instrument shows a wet bias of 5% at 0.30 hPa and a dry bias of −7% at 0.03 hPa. The mean difference between the Onsala instrument and MLS is between −7% at 0.7 hPa and −3% at 0.07 hPa.

[33] The large differences in the standard deviations in Figure 4 are mainly due to differences in the performance of the instruments and to some extent due to the increase in the natural variability with latitude. The standard deviation of variations on time scales of less than 90 days at 0.10 hPa derived from the MLS H_2O data are as follows: Onsala: 11% (0.7 ppm); Bern: 9% (0.6 ppm); Seoul: 7% (0.4 ppm); Mauna Loa: 4% (0.3 ppm); Lauder: 8% (0.5 ppm). The noisy nature of the Bern and Seoul data becomes evident in relation to these numbers and compared to the performance of the Lauder instrument, which shows lower standard deviations and is located at a comparable latitude. At altitudes above the 0.10 hPa level the standard deviations of the Bern and Seoul data are comparable to the natural variability of H_2O, while for the other instruments the scatter is less than the natural variability revealing better correlation with the reference data on time scales below 90 days (not shown). For the Bern instrument the standard deviation is reduced by 20% when the data of the summer time periods are not considered.

[34] The standard deviations of the differences between the ground-based instruments and MLS are a good estimate of their statistical uncertainties. From Figure 4 one can see that the mean differences between the ground-based instruments are smaller than their combined statistical uncertainties. In other words, the ground based instruments do not differ significantly from each other and, in this sense, the five ground-based instruments build a consistent network.

[35] Figure 5 shows time series of H_2O at 0.10 and 0.03 hPa as observed by the ground-based instruments and MLS. The instruments represent well the seasonal cycle in the mesosphere revealing an increase in amplitude toward higher latitudes and also show a lot of small-scale features like planetary waves that are particularly evident at mid and high latitudes during the spring season (Lauder, Bern and Onsala). A secondary wintertime maximum is characteristic for the seasonal cycle in the mesosphere especially at midlatitudes and is well represented in the Bern and Lauder data.

[36] The systems from Bern, Seoul and Lauder generally overestimate the water vapor content during the summer period at 0.10 hPa and thus overestimate the seasonal variations. This is also reflected in Figure 7 that shows the monthly mean differences between the ground-based

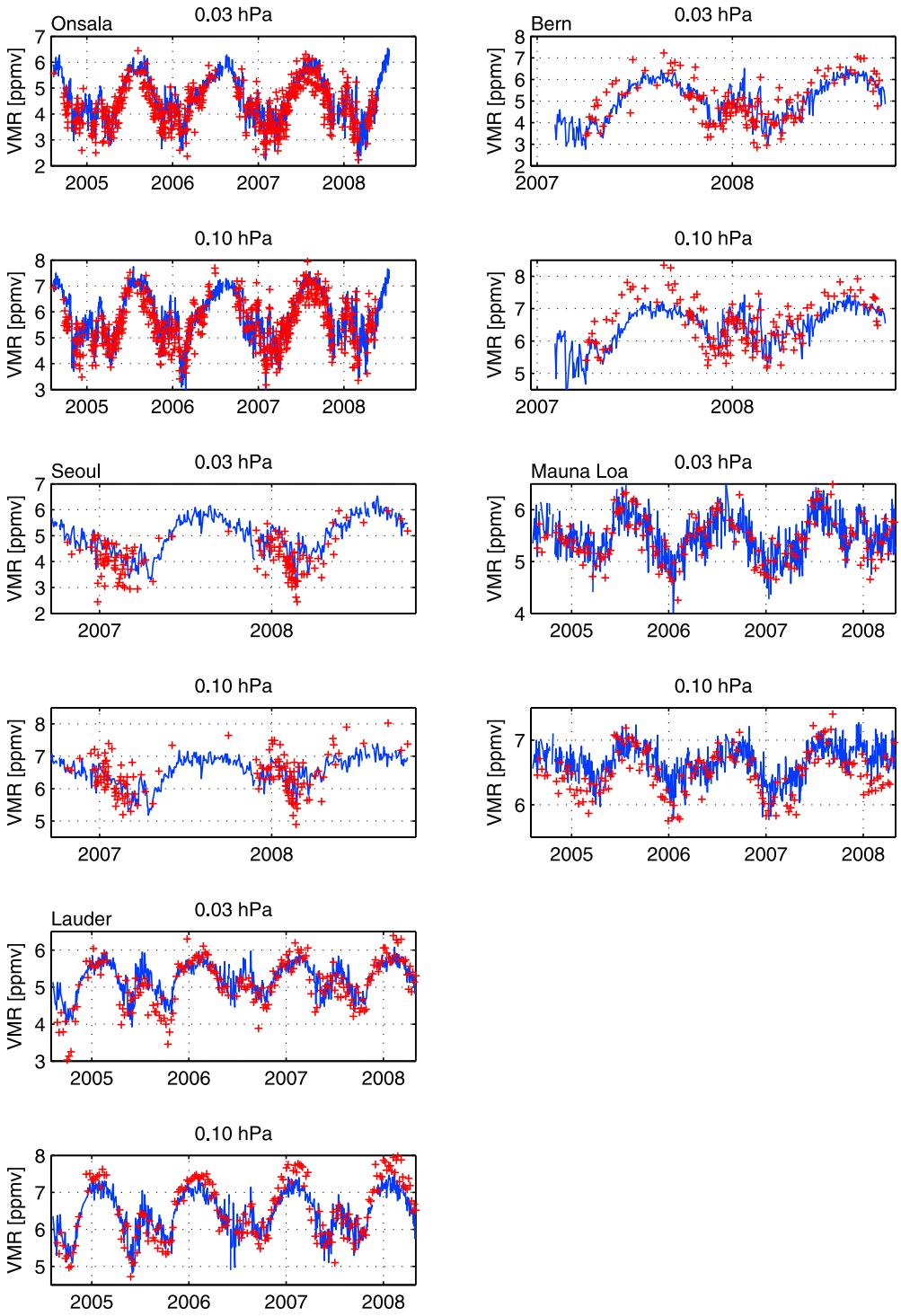

Figure 5. Time series of mesospheric H_2O at 0.10 and 0.03 hPa as observed by the ground-based instruments (red) and MLS (blue). The MLS profiles have been convolved with the averaging kernels of the ground-based instruments to account for differences in vertical resolution and sensitivity.

instruments and the reference since 2004. Please note that in the case of the Seoul system the monthly mean differences for the months May to October are based on single measurements only. Furthermore, Figure 7 reveals that the seasonal amplitude in the monthly mean differences of the Bern instrument could be significantly reduced between 2007 and 2008.

[37] Figure 6 shows time series of stratospheric measurements. Generally the time series of the ground-based instruments become more unstable at these levels which is mainly because baseline artifacts in the spectra start to interfere (see section 5.1). The instruments from Mauna Loa and Lauder perform well at 1 hPa representing nicely the weak seasonal cycle. However, on time scales of weeks not much of the

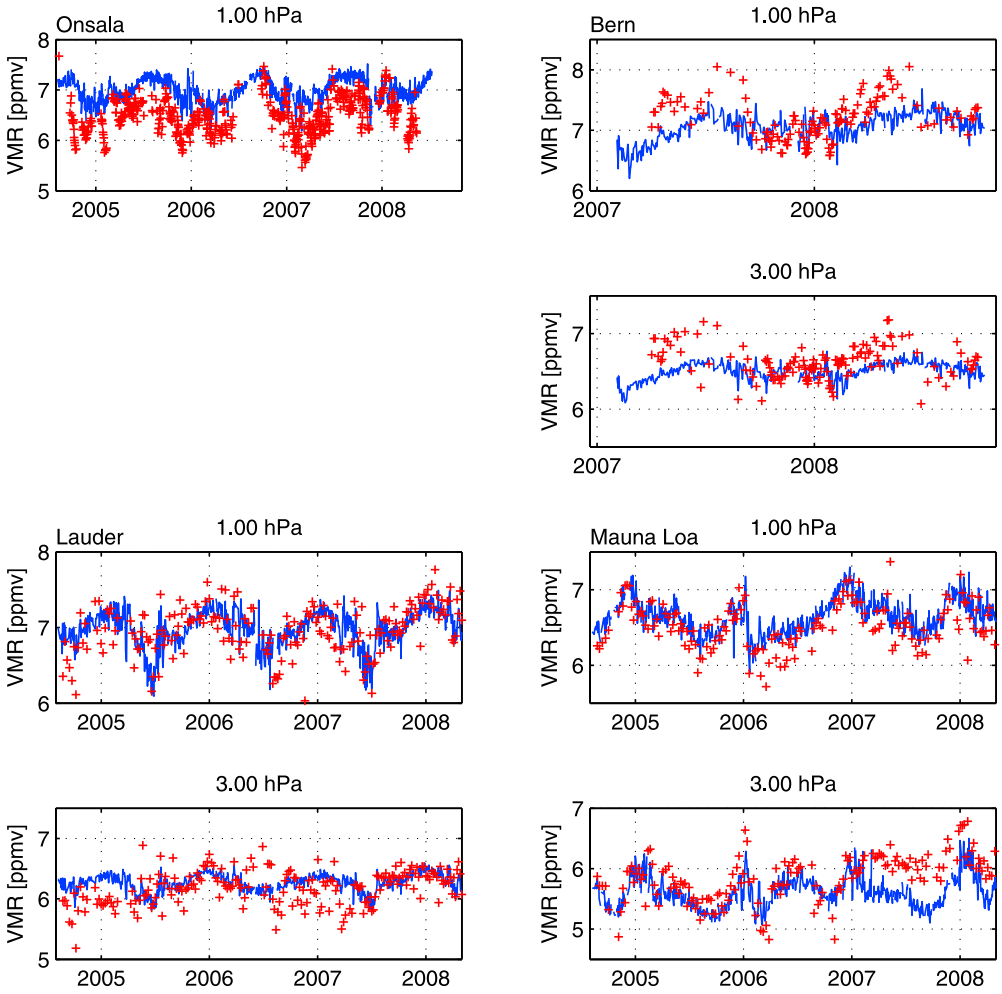

Figure 6. Time series of stratospheric H_2O at 1 and 3 hPa as observed by the ground-based instruments (red) and MLS (blue). The MLS profiles have been convolved with the averaging kernels of the ground-based instruments to account for differences in vertical resolution and sensitivity.

variations can be expected to be real. We would like to emphasize the abrupt drop in the H_2O time series of WVMS and MLS at 1 hPa over Mauna Loa at the beginning of 2006 (see Figure 6). This feature is not present at 3 hPa which demonstrates that these two layers are independent to a great extent. In early 2007 the 3 hPa measurements from Mauna Loa developed a positive bias relative to the MLS measurements which persisted until the end of the time series. If this bias jump is corrected for then the seasonal variations from early 2007 onward at 3 hPa appear reasonable.

[38] The Onsala instrument shows a dry bias and does not catch small-scale features at 1 hPa but the seasonal cycle is apparent. The limited bandwidth of the Onsala system does not allow retrieval of water vapor below 2 hPa. The stratospheric data of the Bern instrument are of good quality during the winter season but show unrealistic fluctuations in summer. This effect is to the largest extent related to the fact that the observation geometry is slightly different in summer to account for the higher opacity. This in turn causes an unfortunate change of the baseline in the calibrated spectra that effectively destroys the retrievals for the stratosphere. This has been recognized recently and in future the change in geometry will be minimized thus allowing reliable retrievals also for the midstratosphere in summer. Due to the limited practical bandwidth we do not show stratospheric measurements from the Seoul system.

7. NDACC Data Set

[39] We have standardized the retrievals as much as possible given differences in receiver and measurement locations. These retrievals will be available for each instrument and the entire measurement time period at www.ndacc.org in their section "Microwave Group," and are processed as described in this paper with one exception. As some of the instrumental records reach farther back than 2004, when MLS started its operation, and as the records of all systems are expected to last for several years no single and continuous global temperature data set exists to be used in the retrievals. We thus created a temperature climatology from the MLS record by building daily averages from the 4 years of observation that are smoothed with an 11 day rectangle filter. The use of this climatology in the retrievals makes the H_2O data of the ground-based instruments independent of any additional information about the state of the atmosphere. While the mean differences between the NDACC

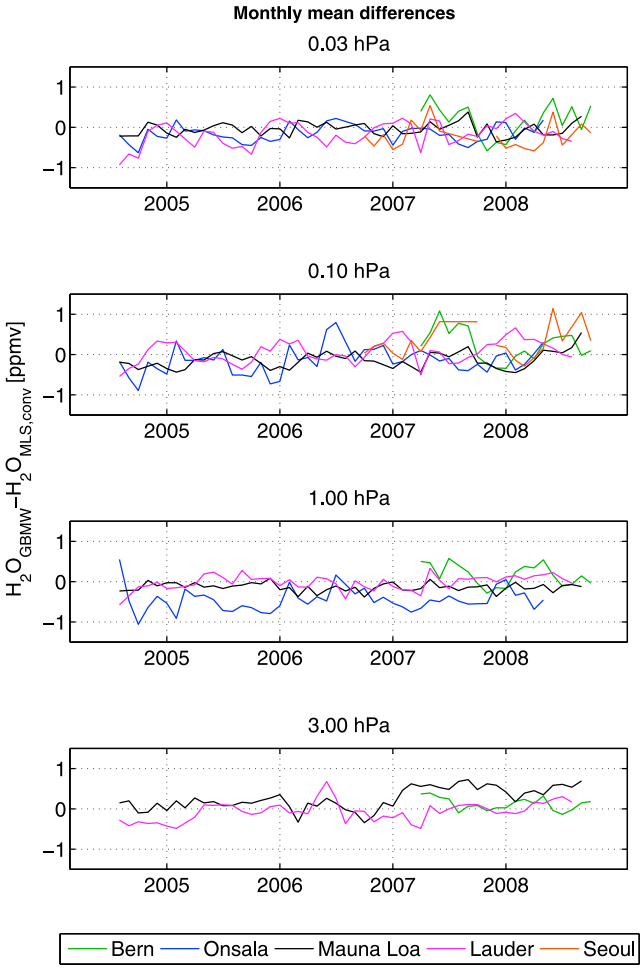

Figure 7. Monthly mean differences between the ground-based instruments and MLS since 2004.

retrievals and MLS are not affected, the standard deviation is slightly degraded for all instruments as H_2O variations on time scales of days and weeks that are accompanied by large variations in temperature cannot be represented correctly using the temperature climatology. Also, any trend in temperature will not be accounted for and could show up as trend in water vapor according to the −2%/5 K error in H_2O. *Remsberg and Deaver* [2005] analyzed HALOE temperature data between 1991 and 2004 and report a linear trend of −0.3 to −1.1 K in the tropical upper stratosphere and the subtropical mesosphere. The solar cycle effect is found to be <1.7 K in the upper stratosphere and mesosphere. *Beig et al.* [2003] present a review of mesospheric temperature trends and summarize that linear trends in the midlatitudinal lower mesosphere are around −2 K/decade. Observations in the polar mesosphere are sparse and the results contradictory. It is thus necessary to assess the temperature climatology in regular intervals and to evaluate, based on recent literature, whether a linear trend should be included.

8. Conclusions

[40] The intercomparison of the five radiometer systems of NDACC with the global measurement from MLS reveals good agreement among the instruments within 10% given that the retrievals of all ground based systems are made with the same spectroscopic parameters and with the same temperature data set. Consistency can be attributed to the network in the sense that the biases between the individual instruments are smaller than their combined statistical uncertainties. This consistency is essential for the network and it allows us to use the measurements of the individual instruments as one single data set.

[41] All instruments show a strong seasonal cycle and planetary-scale wave features in the mesosphere in good agreement with the reference data set from MLS. While the WVMS systems from Lauder and Mauna Loa perform very well in the upper stratosphere, the performance of the other instruments is slightly degraded at 1 hPa. The main reason for this are instrumental instabilities that lead to variations in the baseline (see section 5.1) which in turn disturb the water vapor retrieval at and below the 1 hPa level. This degradation is particularly a problem for the instruments with a low bandwidth (Onsala and Seoul) for which it is difficult to characterize the baseline. Baseline problems become even more evident in the mid stratosphere (3 hPa) and below, where the detection of the seasonal cycle and planetary waves is possible, but where all of the instruments have difficulties to provide stable long-term measurements. Major efforts are being made to improve and understand instrumental stability in order to get stable retrievals in the mid and lower stratosphere.

[42] The compilation of a NDACC data set using a temperature climatology derived from the MLS temperature record shows good consistency within ±10%. It is independent of additional observations or analyses and will be extended into the future and back to 1992 when the WVMS system in Lauder started its operation still allowing to keep the data sets homogeneous.

[43] The overall good performance of this network for middle atmospheric water vapor has been demonstrated and it should become a standard reference for any validation study dealing with water vapor in the stratosphere or mesosphere.

[44] **Acknowledgments.** This work has been supported by the Swiss National Science foundation under grant 200020-115882/1 as well as through the project SHOMING financed by MeteoSwiss within GAW. We acknowledge the support of the European Commission through the GEOMON Integrated Project under the 6th Framework Program (contract FOP6-2005-Global-4-036677) and the support by NASA under the Upper Atmosphere Research Program and by the Naval Research Laboratory. We also would like to thank the teams at Lauder, Mauna Loa, and Seoul for their technical support to run the instruments. Work at the Jet Propulsion Laboratory, California Institute of Technology, was carried out under a contract with the National Aeronautics and Space Administration.

References

Beig, G., et al. (2003), Review of mesospheric temperature trends, *Rev. Geophys.*, *41*(4), 1015, doi:10.1029/2002RG000121.

Buehler, S. A., P. Eriksson, T. Kuhn, A. von Engeln, and C. Verdes (2005), Arts, the atmospheric radiative transfer simulator, *J. Quant. Spectrosc. Radiat. Transfer*, *91*, 65–93.

Cazzoli, G., C. Puzzarini, G. Buffa, and O. Tarrini (2007), Experimental and theoretical investigation on pressure-broadening and pressure-shifting of the 22.2 GHz line of water, *J. Quant. Spectrosc. Radiat. Transfer*, *105*, 438–449.

Cohen, E. A., M. L. Delitsky, J. C. Pearson, H. S. P. Müller, H. M. Pickett, and R. L. Poynter (1998), Submillimeter, millimeter, and microwave spectral line catalog, *J. Quant. Spectrosc. Radiat. Transfer*, *60*, 883–890.

Deuber, B., N. Kämpfer, and D. G. Feist (2004), A new 22-GHz radiometer for middle atmospheric water vapour profile measurements, *IEEE Trans. Geosci. Remote Sens.*, *42*(5), 974–984.

Deuber, B., A. Haefele, D. G. Feist, L. Martin, N. Kämpfer, G. E. Nedoluha, V. Yushkov, S. Khaykin, R. Kivi, and H. Vömel (2005), Middle Atmospheric Water Vapour Radiometer—MIAWARA: Validation and first results of the LAUTLOS/WAVVAP campaign, *J. Geophys. Res.*, *110*, D13306, doi:10.1029/2004JD005543.

De Wachter, E., A. Murk, C. Straub, A. Haefele, S. Ka, J. J. Oh, and N. Kämpfer (2009), Effects of resonances in corrugated horn antennas for a 22 GHz balancing radiometer, *IEEE Geosci. Remote Sens. Lett.*, *6*, 3–7, doi:10.1109/LGRS.2008.2005851.

Eriksson, P., C. Jiménez, and S. A. Buehler (2005), Qpack, a general tool for instrument simulation and retrieval work, *J. Quant. Spectrosc. Radiat. Transfer*, *91*, 47–64.

Forkman, P., P. Eriksson, and A. Winnberg (2003), The 22 GHz radio-aeronomy reciver at Onsala Space Observatory, *J. Quant. Spectrosc. Radiat. Transfer*, *77*, 23–42.

Forster, P., et al. (2007), Changes in atmospheric constituents and in radiative forcing, in *Climate Change 2007: The Physical Science Basis. Contribution of Working Group I to the Fourth Assessment Report of the Intergovernmental Panel on Climate Change*, pp. 131–234, Cambridge Univ. Press, Cambridge, U. K.

Haefele, A., K. Hocke, N. Kämpfer, P. Keckhut, M. Marchand, S. Bekki, B. Morel, T. Egorova, and E. Rozanov (2008), Diurnal changes in middle atmospheric H_2O and O_3: Observations in the Alpine region and climate models, *J. Geophys. Res.*, *113*, D17303, doi:10.1029/2008JD009892.

Han, Y., and E. R. Westwater (2000), Analysis and improvement of tipping calibration for ground-based microwave radiometers, *IEEE Trans. Geosci. Remote Sens.*, *38*, 1260–1276.

Harris, J. E. (1976), The Distribution of water vapor in the stratosphere, *Rev. Geophysics*, *14*, 565–575.

Hocke, K., et al. (2007), Comparison and synergy of stratospheric ozone measurements by satellite limb sounders and the ground-based microwave radiometer SOMORA, *Atmos. Chem. Phys.*, *7*, 4117–4131.

Lambert, A., et al. (2007), Validation of the Aura Microwave Limb Sounder middle atmosphere water vapor and nitrous oxide measurements, *J. Geophys. Res.*, *112*, D24S36, doi:10.1029/2007JD008724.

Liebe, H. J. (1989), MPM—A atmospheric millimeter-wave propagation model, *Int. J. Infrared Millimeter Waves*, *10*, 631–650.

Motte, E., P. Ricaud, M. Niclas, B. Gabard, and F. Gangneron (2007), A 22 GHz mobile microwave radiometer for the study of stratospheric water vapor, paper presented at IGARSS 2007, Inst. of Electr. and Electron. Eng., New York.

Nedoluha, G. E., R. M. Bevilacqua, R. M. Gomez, D. L. Thacker, W. B. Waltman, and T. A. Pauls (1995), Ground-based measurements of water vapor in the middle atmosphere, *J. Geophys. Res.*, *100*(D2), 2927–2939.

Nedoluha, G. E., R. Bevilacqua, R. Gomez, W. Waltman, B. Hicks, D. Thacker, J. Russell III, M. Abrams, H. Pumphrey, and B. Connor (1997), A comparative study of mesospheric water vapor measurements from the ground-based water vapor millimeter-wave spectrometer and space-based instruments, *J. Geophys. Res.*, *102*(D14), 16,647–16,661.

Nedoluha, G. E., R. M. Gomez, B. C. Hicks, R. M. Bevilacqua, J. M. Russell III, B. J. Connor, and A. Lambert (2007), A comparison of middle atmospheric water vapor as measured by WVMS, EOS-MLS, and HALOE, *J. Geophys. Res.*, *112*, D24S39, doi:10.1029/2007JD008757.

Parrish, A., R. L. deZafra, P. M. Solomon, and J. W. Barret (1988), A ground–based technique for millimeter wave spectroscopic observations of stratospheric trace constituents, *Radio Sci.*, *23*, 106–118.

Payne, V. H., J. S. Delamere, K. E. Cady-Pereira, R. R. Gamache, L. J-Moncet, S. Mlawer, and A. Clough (2008), Air-broadened half-widths of the 22- and 183-GHz water-vapor lines, *IEEE Trans. Geosci. Remote Sens.*, *46*, 3601–3617.

Poynter, R. L., and H. M. Pickett (1985), Submillimeter, millimeter, and microwave spectral-line catalog, *Appl. Opt.*, *24*, 2235–2240.

Remsberg, E. E., and L. E. Deaver (2005), Interannual, solar cycle, and trend terms in middle atmospheric temperature time series from HALOE, *J. Geophys. Res.*, *110*, D06106, doi:10.1029/2004JD004905.

Rodgers, C. D. (1976), Retrieval of atmospheric temperature and composition from remote measurements of thermal radiation, *Rev. Geophys.*, *14*, 609–624.

Rothman, L. S., et al. (2005), The HITRAN 2004 molecular spectroscopic database, *J. Quant. Spectrosc. Radiat. Transfer*, *96*, 139–204.

Schwartz, M. J., et al. (2008), Validation of the Aura Microwave Limb Sounder temperature and geopotential height measurements, *J. Geophys. Res.*, *113*, D15S11, doi:10.1029/2007JD008783.

Straub, C., A. Murk, N. Kämpfer, D. Zardet, and B. Stuber (2008), Development of a 22 GHz correlating radiometer for the observation of stratospheric water vapor, paper presented at 2008 Microwave Radiometry and Remote Sensing of the Environment (MICRORAD 2008), IEEE Geosci. and Remote Sens. Soc., New York.

Thacker, D. L., R. M. Bevilacqua, W. B. Waltman, T. A. Pauls, R. M. Gomez, G. E. Nedoluha, and P. R. Schwartz (1995), Ground-based sensing of water-vapor in the stratosphere and mesosphere, *IEEE Trans. Instrum. Meas.*, *44*(2), 355–359.

Vömel, H., et al. (2007), Validation of Aura MLS water vapor by balloon-borne Cryogenic Frost point Hygrometer measurements, *J. Geophys. Res.*, *112*, D24S37, doi:10.1029/2007JD008698.

Waters, J. W., et al. (2006), The Eartch Observing System Microwave Limb Sounder (EOS MLS)on the Aura satellite, *IEEE Trans. Geosci. Remote Sens.*, *44*, 1075–1092.

E. De Wachter, A. Haefele, K. Hocke, and N. Kämpfer, Department of Microwave Physics, Institute of Applied Physics, University of Bern, Sidlerstrasse 5, Bern CH-3012, Switzerland. (haefele@iap.unibe.ch)

P. Eriksson and P. Forkman, Department of Radio and Space Science, Chalmers University of Technology, Gothenburg S-41296, Sweden.

R. M. Gomez and G. E. Nedoluha, Naval Research Laboratory, 4555 Overlook Ave., SW, Washington, DC 20375, USA.

A. Lambert and M. J. Schwartz, Jet Propulsion Laboratory, California Institute of Technology, Pasadena, CA 91109, USA.